

## Avalanches in 2D Dislocation Systems: Plastic Yielding Is Not Depinning

Péter Dusán Ispánovity,<sup>1,\*</sup> Lasse Laurson,<sup>2</sup> Michael Zaiser,<sup>3</sup> István Groma,<sup>1</sup> Stefano Zapperi,<sup>4</sup> and Mikko J. Alava<sup>2</sup>

<sup>1</sup>*Department of Materials Physics, Eötvös University Budapest, H-1117 Budapest, Pázmány Péter Sétány 1/a, Hungary*

<sup>2</sup>*COMP Centre of Excellence, Department of Applied Physics, Aalto University,  
P.O. Box 11100, FIN-00076 Aalto, Espoo, Finland*

<sup>3</sup>*Institute of Materials Simulation, Department of Materials Science, University of Erlangen-Nürnberg,  
Dr.-Mack-Strasse 77, 90762 Fürth, Germany*

<sup>4</sup>*CNR-IENI, Via R. Cozzi 53, 20125 Milano, Italy and ISI Foundation, Via Alassio 11/C, 10126 Torino, Italy*

(Received 12 July 2013; revised manuscript received 14 May 2014; published 13 June 2014)

We study the properties of strain bursts (dislocation avalanches) occurring in two-dimensional discrete dislocation dynamics models under quasistatic stress-controlled loading. Contrary to previous suggestions, the avalanche statistics differ fundamentally from predictions obtained for the depinning of elastic manifolds in quenched random media. Instead, we find an exponent  $\tau = 1$  of the power-law distribution of slip or released energy, with a cutoff that increases exponentially with the applied stress and diverges with system size at all stresses. These observations demonstrate that the avalanche dynamics of 2D dislocation systems is scale-free at every applied stress and, therefore, cannot be envisaged in terms of critical behavior associated with a depinning transition.

DOI: 10.1103/PhysRevLett.112.235501

PACS numbers: 81.40.Lm, 61.72.Lk, 68.35.Rh, 81.05.Kf

Crystalline solids subject to an increasing stress undergo a transition (“yielding”) from nearly elastic behavior to plastic flow by collective dislocation motion. Both during the runup to yielding and in the subsequent plastic flow regime, dislocation systems exhibit strongly intermittent, avalanchelike dynamics. In micron-sized specimens these avalanches show as abrupt strain bursts with a broad, power law—type size distribution [1–3], and in larger samples they manifest themselves through acoustic emission events with power-law distributed amplitudes [4,5].

Several researchers have advanced the idea that the dislocations in a crystal deforming under stress might be envisaged as a driven nonequilibrium system, where power-law distributed avalanches arise from dynamic critical behavior associated with a nonequilibrium phase transition at a critical value  $\sigma_{\text{ext}} = \sigma_c$  of the externally applied stress, analogous to the depinning transition of elastic interfaces in random media [6]. This idea applies in a straightforward manner to single dislocations interacting with immobile impurities which provide a textbook example of one-dimensional elastic manifolds undergoing a depinning transition [7,8]. In generalization of this observation, several authors have argued that the mean-field limit of the depinning transition might correctly describe the dynamics of stress-driven many-dislocation systems even when other defects are absent [9–14]. In this picture plastic yielding is envisaged as a continuous phase transition where the external stress acts as control parameter and a critical point is reached at the yield stress. There are several motivations for such an analogy: (i) dislocation-dislocation interactions are long range, implying that a mean-field description could be applicable, and (ii) the strain burst distribution appears to be a power law,  $P(\Delta\gamma) \propto \Delta\gamma^{-\tau}$ , with

$\tau$  found to be  $\tau \approx 1.5$  both experimentally and numerically [1,2,15–17], in apparent agreement with mean-field depinning (MFD) [6].

There are, however, several unresolved issues regarding the validity of the depinning picture. In the classical depinning scenario, an elastic manifold interacts with a *static* (quenched) pinning field representing immobile impurities of the medium. However, yielding and avalanche dynamics of plastic flow are generic features of crystal plasticity that do not require impurities or other types of quenched disorder. Discrete dislocation dynamics (DDD) models [18–24], which are commonly used to model plasticity of pure fcc crystals, relate the yield stress to the mutual trapping (or *jamming* [22,23]) which occurs as interacting dislocations form complex metastable structures even in the absence of other defects [2,5,22,25]. This important difference is illustrated schematically in Fig. 1.

Even if we consider the dynamics of the simplest possible DDD model—a 2D system of straight parallel dislocations moving on a single slip system—there are several findings that are not consistent with MFD. These include the following. (i) For the relaxation exponent of the Andrade creep law, i.e., the initial power-law decay of the mean strain rate under constant applied stress,  $\langle \dot{\gamma}(t) \rangle \propto t^{-\theta}$ , one finds  $\theta \approx 2/3$  [22,26], whereas MFD predicts  $\theta = 1$  for the critical relaxation of the order parameter [6,27]. (ii) Temporal scaling of the spatial fluctuations of the local creep rates indicates non-mean-field behavior [28]. (iii) The duration of the power-law relaxation regime is at low stresses limited by the system size rather than by the distance  $\sigma_c - \sigma_{\text{ext}}$  from the critical point [26], again inconsistent with depinning. (iv) The response to cyclic applied stresses is not consistent with MFD [29]. (v) The

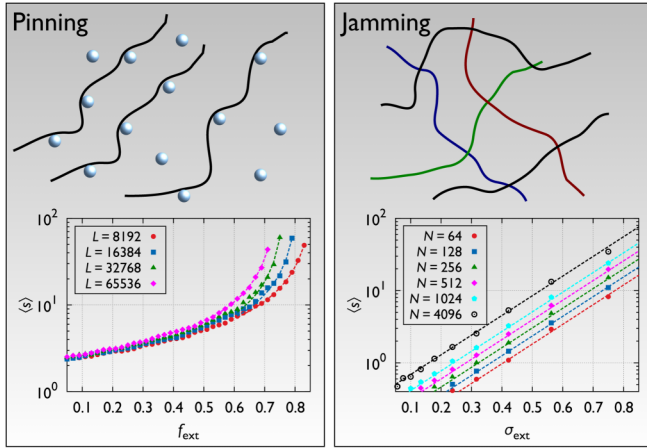


FIG. 1 (color online). Differences between pinning and the present jamming scenario. Pinning is induced by quenched disorder, which stops the motion of driven elastic manifolds for applied forces  $f_{\text{ext}}$  below a critical value  $f_c$  (top left). With  $f_{\text{ext}}$  approaching  $f_c$  from below, the manifold moves ahead in avalanches with an average avalanche size  $\langle s \rangle$  which in MFD diverges as  $\langle s \rangle \propto [f_c(L) - f_{\text{ext}}]^{-1}$  (1D elastic manifold with elastic interactions decaying as  $1/r$ , bottom left).  $f_c$  depends on the system size  $L$  due to finite size scaling,  $f_c(L) = f_c(\infty) + aL^{-1}$ . In a dislocation system without quenched disorder, dislocation motion may stop due to formation of jammed configurations (top right). The behavior of  $\langle s \rangle$  we observe in this case is fundamentally different from the depinning scenario, with  $\langle s \rangle = A(N)e^{\sigma_{\text{ext}}/\sigma_0}$ , where  $A(N)$  grows with the number of dislocations  $N$  (bottom right).

stress dependence of the steady state strain rate obeys  $\langle \dot{\gamma} \rangle \propto (\sigma_{\text{ext}} - \sigma_c)^\beta$ . For the exponent  $\beta$ , MFD predicts  $\beta = 1$  [6], but  $\beta \approx 1.8$  was measured by DDD simulations [22]. With a different methodology, however,  $\beta \approx 1$  was found recently for DDD systems, too [14].

Finally, we note that comparisons between theoretical and experimental values of avalanche exponents might be misleading, since most studies of dislocation avalanche statistics consider aggregate distributions (integrated over the different  $\sigma_{\text{ext}}$  values), whereas the theoretical MFD prediction  $\tau = 1.5$  refers to stress-resolved distributions [30], so the numerical and experimental findings of  $\tau \approx 1.5$  by themselves do not provide strong evidence for the MFD scenario.

In this Letter, we report results of quasistatic stress-controlled simulations of 2D DDD models and demonstrate that the stress-resolved avalanche statistics do not follow the MFD predictions. To underline the general nature of our findings, we consider a continuous time dynamics (CTD) model with continuous spatial resolution together with two cellular automaton (CA) models, finding the same results in all cases.

The DDD models considered here are minimal representations of dislocation systems, consisting of straight

parallel edge dislocations moving on a single slip system. This implies that the problem reduces to the dynamics of 2D systems of pointlike objects (the intersection points of the dislocation lines with a perpendicular plane) which move on parallel lines in the  $x$  direction of a 2D Cartesian coordinate system. We consider simulation areas of size  $L \times L$  containing  $N$  dislocations with Burgers vectors  $\mathbf{b}_i = s_i(b, 0)$ , where  $s_i \in \{1, -1\}$  and  $i \in [1 \dots N]$ . We assume equal numbers of dislocations of positive and negative signs. The CTD equations of motion read

$$\dot{x}_i = Mbs_i \left[ \sum_{j \neq i} s_j \sigma_{\text{ind}}(\mathbf{r}_i - \mathbf{r}_j) + \sigma_{\text{ext}} \right], \quad \dot{y}_i = 0. \quad (1)$$

Here  $M$  is the dislocation mobility,  $\sigma_{\text{ind}}(\mathbf{r}) = Gb \cos(\phi) \cos(2\phi)r^{-1}$  is the shear stress field of an individual dislocation (with periodic boundary conditions assumed in both directions [31]),  $G$  is an appropriate elastic constant, and  $\sigma_{\text{ext}}$  is the external shear stress. The CA models are defined by discretizing the system in both space and time. Dislocations are allowed to move from one cell to a neighboring cell if such a move decreases the elastic energy of the system. We apply two different rules for the dynamics: (i) In extremal dynamics (ED) at each step only the move that produces the largest energy decrease is carried out; (ii) in random dynamics (RD) the moved dislocation is selected randomly from those that are allowed to move. The motivation of using all these models together is to test the generality of our results by comparing the linear force-velocity characteristics of the CTD model, Eq. (1), with two different highly nonlinear relations of the CA models. The CTD corresponds to easy glide at intermediate temperatures, where thermal activation and dislocation climb are negligible, ED is a low temperature limit for thermally activated glide, and RD is an artificial law differing fundamentally from both CTD and ED. In what follows, we measure lengths, times, and stresses in units of  $\rho^{-0.5}$ ,  $(\rho M G b^2)^{-1}$ , and  $G b \rho^{0.5}$ , respectively, with  $\rho = N/L^2$  the dislocation density [32].

A quasistatic stress-controlled loading protocol is implemented as follows. First, a random initial dislocation configuration is let to relax at  $\sigma_{\text{ext}} = 0$ . Then, for the CTD model,  $\sigma_{\text{ext}}$  is increased at a slow rate from zero until the average dislocation velocity  $V(t) = (1/N) \sum_i |\dot{x}_i(t)|$  exceeds a small threshold value  $V_{\text{th}}$ . While  $V(t) > V_{\text{th}}$  and an avalanche propagates, the external stress is kept constant, and the amount of slip  $s = \sum_i s_i \Delta x_i$  and plastic strain  $\Delta \gamma = s/L^2$  produced within the avalanche are recorded. Here  $\Delta x_i$  denotes the displacement of the  $i$ th dislocation during the given avalanche. After the avalanche is finished [ $V(t) < V_{\text{th}}$ ], the external stress is again increased at a slow rate until the next avalanche is triggered. A similar loading protocol is implemented in the CA models: In between the avalanches, the external stress is increased just enough to make exactly one dislocation

TABLE I. Parameters of Eqs. (2) and (3) obtained by fitting to the numerically obtained avalanche distributions.

Model	$\tau$	$\beta$	$\sigma_0$
CTD	$0.97 \pm 0.03$	$0.36 \pm 0.04$	$0.07 \pm 0.01$
CA with ED	$1.00 \pm 0.03$	$0.36 \pm 0.02$	$0.116 \pm 0.004$
CA with RD	$1.02 \pm 0.01$	$0.44 \pm 0.01$	$0.122 \pm 0.002$

move, which then may trigger further dislocation activity, during which the applied stress is again kept constant. We have checked the robustness of the results against different loading protocols (e.g., first relaxing the system under a nonvanishing stress and then slowly increasing the stress) finding no quantitative differences.

For each model, we consider the avalanche size distribution  $P(s)$  at different levels of the external stress below the yield stress. For  $s > 1$  (i.e., slip events larger than that corresponding to a single dislocation moving one average dislocation spacing), these can be well characterized by a power law with a cutoff,

$$P(s) \propto s^{-\tau} f(s/s_0). \quad (2)$$

To estimate  $\tau$  and  $s_0$ , a fitting procedure has been used that fits Eq. (2) simultaneously to the avalanche distributions obtained at different stress levels and system sizes. The cutoff was found to follow

$$s_0(\sigma_{\text{ext}}, N) \propto N^\beta \exp(\sigma_{\text{ext}}/\sigma_0). \quad (3)$$

Table I shows the parameters obtained by fitting Eqs. (2) and (3) to the avalanche size distributions. Figures 2(a)–(c) show the  $P(s)$  distributions for the three models plotted as functions of  $s/s_0$ . The validity of Eq. (3) is demonstrated by the collapse of all distributions in the cutoff region. Since Eq. (2) holds only for  $s > 1$ , the curves follow the master curve only as long as  $s/s_0 > 1/s_0$ , thus over longer range as the applied stress and/or the system size increase. Below this regime the behavior is governed by the single-dislocation dynamics and therefore differs between the three models.

The observations summarized by Eqs. (2) and (3) and Table I exhibit several interesting features which are the main results of this Letter.

(i) The power-law exponent  $\tau$  has the value  $\tau \approx 1.0$ , clearly different from the MFD value  $\tau = 1.5$ . According to

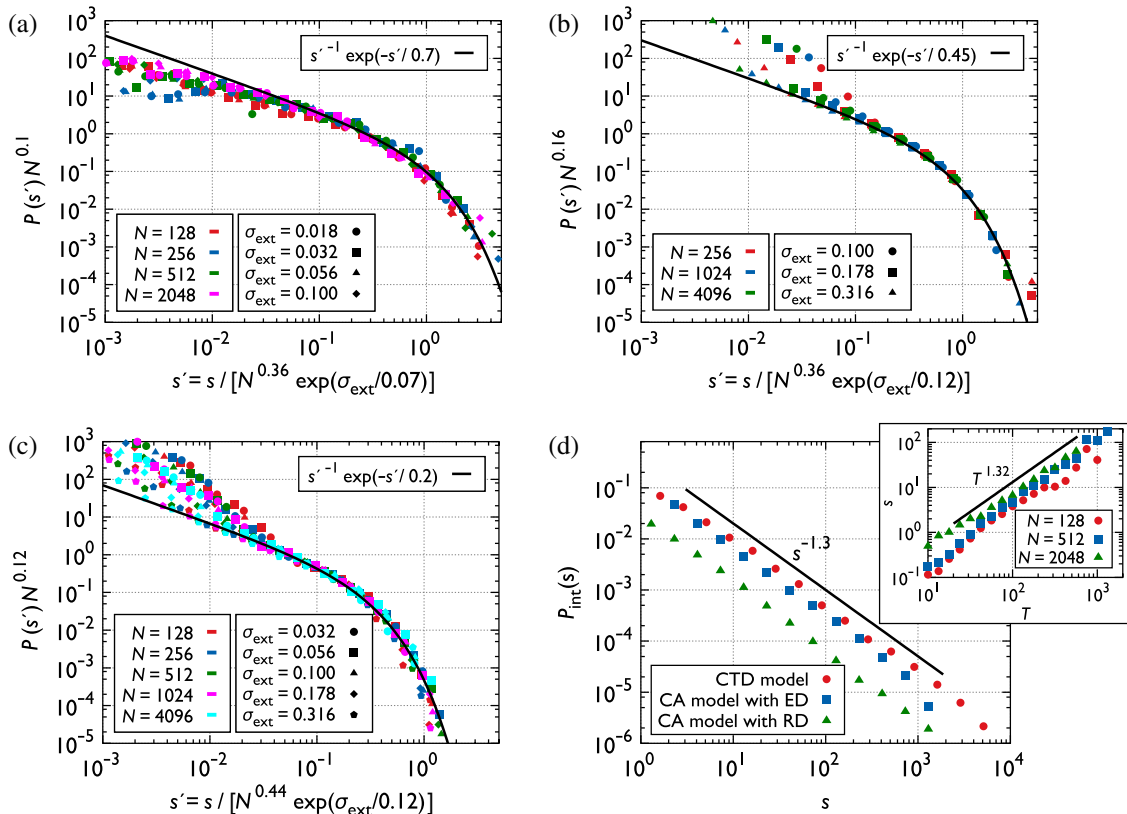


FIG. 2 (color online). (a)–(c) Stress-resolved distributions of avalanche sizes for the various DDD models at different applied stresses and system sizes. The distributions are plotted as functions of  $s' := s/s_0$ , with  $s_0$  obeying Eq. (3). (a) CTD model, (b) CA model with ED, (c) CA model with RD. (d) Aggregate avalanche size distributions  $P_{\text{int}}$  integrated over  $\sigma_{\text{ext}}$  for system sizes  $N = 512$  (CTD model) and  $N = 4096$  (CA models). Inset: Scaling of the avalanche size  $s$  with the duration  $T$  in the CTD model, for three different system sizes  $N$ .

Fig. 2(d), the integrated distribution (where avalanches with all stress values are considered together) exhibits a larger exponent  $\tau_{\text{int}} \approx 1.3$ , in line with a recent reanalysis of experimental micropillar compression data [33]. Moreover, the inset of Fig. 2(d) shows that in the CTD model the avalanche size scales with the duration as  $s \propto T^\gamma$ , with  $\gamma \approx 1.32$  clearly different from the MFD value of 2.

(ii) According to Eq. (3), the cutoff  $s_0$  increases with system size even at very small applied stress like  $s_0 \propto N^\beta$  with  $\beta \approx 0.4$ .

(iii) The cutoff  $s_0$  does not diverge at a certain external stress, rather it exhibits an exponential stress dependence.

The fundamental difference between the present and depinning behavior is highlighted in Fig. 1, where the average avalanche size is compared for the CA DDD model with ED and a simple depinning model. In the latter an elastic line with  $1/r$ -type self-interaction is driven through a random pinning field [34].

Equation (3) implies that the cutoff of the plastic strain bursts  $\Delta\gamma$  scales as  $\Delta\gamma_0 = s_0/L^2 \propto N^{\beta-1} = L^{2\beta-2}$ . Since  $\beta < 1$ , with increasing system size the plastic strain events get smaller, in line with the experimental evidence that macroscopic plasticity is a smooth process. We note that a similar scaling form (with  $\beta \approx 0.5$ ) has been proposed for systems deforming in the strain hardening regime above the yield stress [2,35]. The remarkable new finding here is that the same scaling also holds for very small stresses far below the yielding threshold. Furthermore, the energy dissipated during an avalanche (at a given external stress) scales as  $E \propto \sigma_{\text{ext}} \Delta\gamma L^2 = \sigma_{\text{ext}} s$  [9]; i.e., it diverges for large specimens at any applied stress. This is in accordance with acoustic emission results obtained during creep experiments on large ice single crystals showing that, even for resolved shear stresses far below the yield stress, the energy  $E$  of the acoustic events exhibits a power-law distribution that spans more than 6 orders of magnitude without any apparent cutoff [4,5]. It needs to be mentioned, that the measured power-law exponent  $\kappa_E$  is larger than the one obtained in this Letter ( $\kappa_E \approx 1.6$  opposed to  $\tau_{\text{int}} \approx 1.3$ ), but since no experimental evidence supports  $E \propto \Delta\gamma$ , such an equality does not necessarily hold.

Thus, our results demonstrate that there are system size effects at every stress level. To understand their origin we consider dynamic correlations in the motion of dislocations. To this end, we analyze the spatial structure of the avalanches in terms of the average spatial distribution of the plastic strain  $\gamma(\mathbf{r})$  produced during an avalanche and its angular average  $\gamma(r)$  [these quantities relate to the avalanche size by  $s = \int \gamma(\mathbf{r}) d^2r = \int 2\pi r \gamma(r) dr$ ]. To determine average values of these quantities, we shift the avalanche initiation points (taken to be the location of the fastest dislocation when  $V_{\text{th}}$  is exceeded) into the origin of a Cartesian coordinate system and then average the superimposed strain patterns over multiple avalanches. Figure 3 demonstrates that  $\gamma(\mathbf{r})$  exhibits a strongly

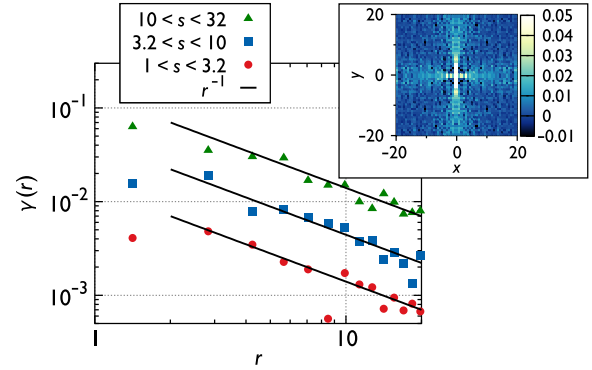


FIG. 3 (color online). Average spatial distribution of the avalanche plastic strain determined for avalanches occurring at  $\sigma_{\text{ext}} \approx 0.08$  in the CTD model for  $N = 2048$ . Main figure: Radial decay of the angle-averaged plastic strain for avalanches of different sizes. Inset: Strain pattern  $\gamma(\mathbf{r})$  averaged over all avalanches.

anisotropic structure and decays slowly along the  $x$  and  $y$  axes. Averaged over all directions, the radial decay is of  $1/r$  type regardless of the avalanche size  $s$ . This indicates that the long-range stress fields of the moving dislocations are not fully screened (contrary to what is observed in equilibrium [36,37]), leading to highly nonlocal spreading of avalanches. Thus, even at low stresses avalanches are influenced by the finite system size, naturally leading to an  $L$ -dependent slip avalanche cutoff. The fact that this cutoff diverges with increasing  $L$  indicates that in the thermodynamic limit the system is scale-free in the dynamic sense even for small applied stresses. Analogous conclusions were drawn regarding the time scales of this system by investigating various relaxation scenarios [26].

To conclude, we have established that the statistics of slip avalanches in simple 2D DDD models is inconsistent with a depinning transition. Fundamental differences between the behavior of dislocation systems and the interface depinning scenario are manifested by the behavior of the cutoff of the avalanche size distribution which, rather than diverging at some critical stress  $\sigma_c$ , scales exponentially with stress but diverges with system size at every stress. In addition, the avalanche exponent  $\tau \approx 1.0$  is inconsistent with MFD. These scale-free properties add to other typical glassy features observed for dislocations, such as slow relaxation [26,32,38] and aging [39].

While we have demonstrated that the equation yielding = depinning is not generally valid, it is important to note that real dislocation systems are composed of flexible lines moving in three dimensions and their behavior may differ from the present, highly idealized 2D models. In addition, in this Letter pure crystals were considered, but a high level of a quenched pinning field (such as impurities) may change the behavior [40]. At larger stresses or strains further phenomena may affect the dynamics of the system, such as thermal effects or the

formation of various dislocation patterns. In conclusion, both 3D DDD simulations and experimental studies with large statistical samples are required in order to understand dislocation avalanches in 3D and to settle the question regarding the fundamental nature of the yielding or jamming transition of dislocation systems.

This work has been supported by the Hungarian Scientific and Research Fund (P.D.I. and I.G., Project No. OTKA-PD-105256 and No. OTKA-K-105335); the European Commission (P.D.I., Project No. MC-CIG-321842); and the Academy of Finland through a Postdoctoral Researcher's Project (L.L., Project No. 139132), through an Academy Research Fellowship (L.L., Project No. 268302), through the Centres of Excellence Program (Project No. 251748), and via two travel grants (L.L., P.D.I., Grants No. 261262 and No. 261521). The numerical simulations were partly performed using computer resources within the Aalto University School of Science "Science-IT" project. S.Z. is supported by the European Research Council, AdG2001-SIZEEFFECTS, and acknowledges support by the visiting professor program of Aalto University.

\*Corresponding author.

ispanovity@metal.elte.hu

- [1] D. M. Dimiduk, C. Woodward, R. LeSar, and M. D. Uchic, *Science* **312**, 1188 (2006).
- [2] F. F. Csikor, C. Motz, D. Weygand, M. Zaiser, and S. Zapperi, *Science* **318**, 251 (2007).
- [3] M. D. Uchic, P. A. Shade, and D. M. Dimiduk, *Annu. Rev. Mater. Res.* **39**, 361 (2009).
- [4] J. Weiss and J.-R. Grasso, *J. Phys. Chem. B* **101**, 6113 (1997).
- [5] M.-C. Miguel, A. Vespignani, S. Zapperi, J. Weiss, and J. R. Grasso, *Nature (London)* **410**, 667 (2001).
- [6] D. S. Fisher, *Phys. Rep.* **301**, 113 (1998).
- [7] S. Zapperi and M. Zaiser, *Mater. Sci. Eng. A* **309–310**, 348 (2001).
- [8] B. Bakó, D. Weygand, M. Samaras, W. Hoffelner, and M. Zaiser, *Phys. Rev. B* **78**, 144104 (2008).
- [9] M. Zaiser and P. Moretti, *J. Stat. Mech.* (2005) P08004.
- [10] M. Zaiser, *Adv. Phys.* **55**, 185 (2006).
- [11] K. A. Dahmen, Y. Ben-Zion, and J. T. Uhl, *Phys. Rev. Lett.* **102**, 175501 (2009).
- [12] N. Friedman, A. T. Jennings, G. Tsekenis, J.-Y. Kim, M. Tao, J. T. Uhl, J. R. Greer, and K. A. Dahmen, *Phys. Rev. Lett.* **109**, 095507 (2012).
- [13] P. M. Derlet and R. Maaß, *Model. Simul. Mater. Sci. Eng.* **21**, 035007 (2013).
- [14] G. Tsekenis, J. T. Uhl, N. Goldenfeld, and K. A. Dahmen, *Europhys. Lett.* **101**, 36003 (2013).
- [15] K. S. Ng and A. H. W. Ngan, *Acta Mater.* **56**, 1712 (2008).
- [16] S. Brinckmann, J.-Y. Kim, and J. R. Greer, *Phys. Rev. Lett.* **100**, 155502 (2008).
- [17] M. Zaiser, J. Schwerdtfeger, A. S. Schneider, C. P. Frick, B. G. Clark, P. A. Gruber, and E. Arzt, *Philos. Mag.* **88**, 3861 (2008).
- [18] D. Weygand, L. H. Friedman, E. Van der Giessen, and A. Needleman, *Model. Simul. Mater. Sci. Eng.* **10**, 437 (2002).
- [19] R. Mader, B. Devincere, and L. P. Kubin, *Phys. Rev. Lett.* **89**, 255508 (2002).
- [20] A. Arsenlis, W. Cai, M. Tang, M. Rhee, T. Opperstrup, G. Hommes, T. G. Pierce, and V. V. Bulatov, *Model. Simul. Mater. Sci. Eng.* **15**, 553 (2007).
- [21] J. A. El-Awady, S. Bulent Biner, and N. M. Ghoniem, *J. Mech. Phys. Solids* **56**, 2019 (2008).
- [22] M. Carmen Miguel, A. Vespignani, M. Zaiser, and S. Zapperi, *Phys. Rev. Lett.* **89**, 165501 (2002).
- [23] L. Laurson, M. Carmen Miguel, and M. J. Alava, *Phys. Rev. Lett.* **105**, 015501 (2010).
- [24] S. M. Keralavarma, T. Cagin, A. Arsenlis, and A. A. Benzerga, *Phys. Rev. Lett.* **109**, 265504 (2012).
- [25] V. V. Bulatov, L. L. Hsiung, M. Tang, A. Arsenlis, M. C. Bartelt, W. Cai, J. N. Florando, M. Hiratani, M. Rhee, G. Hommes, T. G. Pierce, and T. D. de la Rubia, *Nature (London)* **440**, 1174 (2006).
- [26] P. D. Ispánovity, I. Groma, G. Györgyi, P. Szabó, and W. Hoffelner, *Phys. Rev. Lett.* **107**, 085506 (2011).
- [27] P. Moretti, M. Carmen Miguel, M. Zaiser, and S. Zapperi, *Phys. Rev. B* **69**, 214103 (2004).
- [28] J. Rosti, J. Koivisto, L. Laurson, and M. J. Alava, *Phys. Rev. Lett.* **105**, 100601 (2010).
- [29] L. Laurson and M. J. Alava, *Phys. Rev. Lett.* **109**, 155504 (2012).
- [30] G. Durin and S. Zapperi, *J. Stat. Mech.* (2006) P01002.
- [31] B. Bakó, I. Groma, G. Györgyi, and G. Zimányi, *Comput. Mater. Sci.* **38**, 22 (2006).
- [32] F. F. Csikor, M. Zaiser, P. D. Ispánovity, and I. Groma, *J. Stat. Mech.* (2009) P03036.
- [33] X. Zhang, B. Pan, and F. Shang, *Europhys. Lett.* **100**, 16005 (2012).
- [34] We note that in the depinning simulations replacing the random pinning potential with a periodic pinning field with a random phase does not change the qualitative features of the depinning transition; see the left-hand panel of Fig. 1.
- [35] M. Zaiser and N. Nikitas, *J. Stat. Mech.* (2007) P04013.
- [36] M. Zaiser, M. Carmen Miguel, and I. Groma, *Phys. Rev. B* **64**, 224102 (2001).
- [37] I. Groma, G. Györgyi, and B. Kocsis, *Phys. Rev. Lett.* **96**, 165503 (2006).
- [38] F. F. Csikor, B. Kocsis, B. Bakó, and I. Groma, *Mater. Sci. Eng. A* **400–401**, 214 (2005).
- [39] B. Bakó, I. Groma, G. Györgyi, and G. T. Zimányi, *Phys. Rev. Lett.* **98**, 075701 (2007).
- [40] M. Ovaska, L. Laurson, and M. J. Alava, arXiv:1401.6315.